Volume 47
Number 10
14 March 2023
Pages 4589–5070

NJC

New Journal of Chemistry

A journal for new directions in chemistry

rsc.li/njc

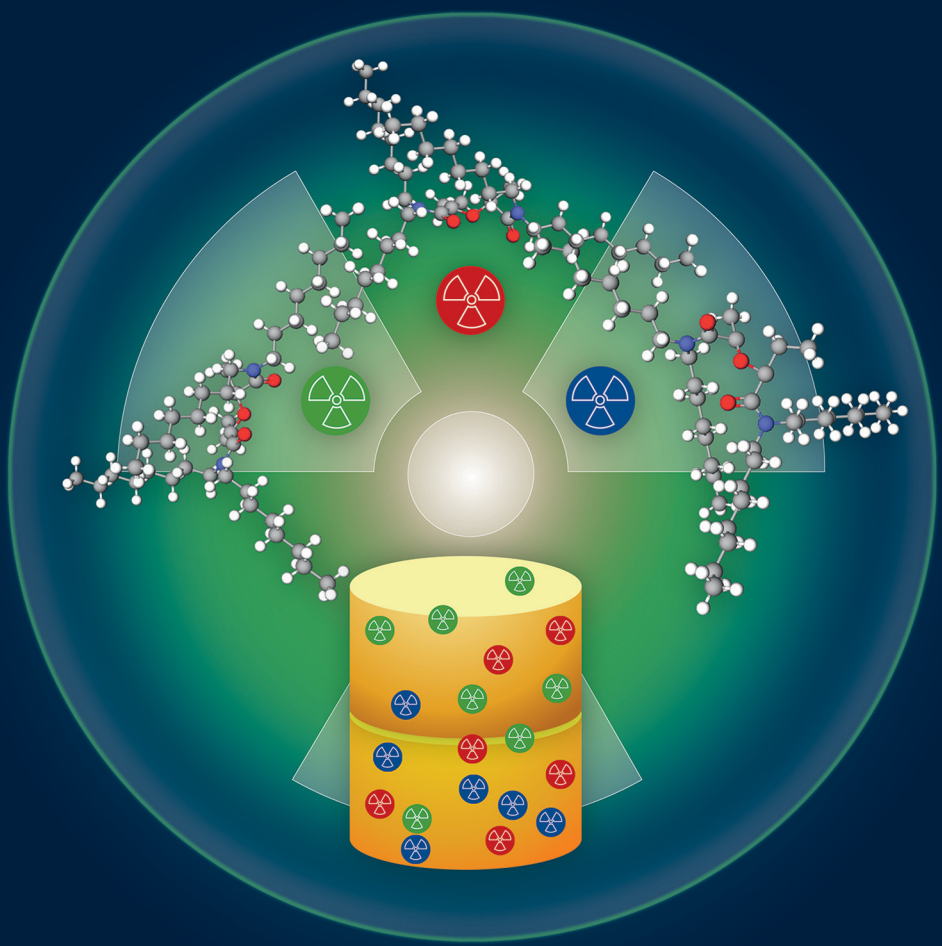

ISSN 1144-0546

ROYAL SOCIETY OF CHEMISTRY

PAPER

Andreas Wilden *et al.*

Synthesis and evaluation of new modified diglycolamides with different stereochemistry for extraction of tri- and tetravalent metal ions

cnrs

NJC

ROYAL SOCIETY OF CHEMISTRY

PAPER

View Article Online
View Journal | View Issue

Cite this: *New J. Chem.*, 2023, **47**, 4619

Synthesis and evaluation of new modified diglycolamides with different stereochemistry for extraction of tri- and tetravalent metal ions†

Laura Diaz Gomez, [a] Andreas Wilden, *[a] Dimitri Schneider, [a] Zaina Paparigas, [a] Giuseppe Modolo, [a] Maria Chiara Gullo, [b] Jurriaan Huskens [b] and Willem Verboom [b]

Americium separation from high level nuclear waste can provide certain benefits such as reducing the long-term heat generation or the possibility of re-use as fuel in innovative reactors. The separation is carried out through solvent extraction. Among commonly used ligands, diglycolamide (DGA) derivatives have shown high distribution ratios for trivalent lanthanides (Ln(III)) and actinides (An(III)). Recently, different diastereomers of DGAs with substitutions in the backbone have shown an inverse selectivity for Am over Cm, in comparison with commonly used DGAs. Hence, we synthesised, characterized, and tested novel *syn*- and *anti*-diastereomers of tetra-*n*-octyl and tetra-*n*-decyl DGAs with two propyl and ethyl-methyl substituents at the backbone methylene carbon atoms. The distribution ratios for An(III) and Ln(III) were found to be generally lower than for the unsubstituted parent molecules due to steric hindrance. On the other hand, ^{239}Pu was much better extracted. All tested ligands showed the inverse selectivity for Am with an Am/Cm separation factor ($SF_{Am/Cm}$) around 1.5. Finally, slope analysis confirmed a 1 : 3 metal : ligand ratio for the DGA complexes.

Received 18th November 2022,
Accepted 11th January 2023

DOI: 10.1039/d2nj05663a

rsc.li/njc

Introduction

Numerous processes (*e.g.*, innovative-SANEX,[1] AmSel,[2] GANEX,[3–5] *etc.*[6,7]) have been developed with the main purpose of minimizing the radiotoxicity of High-Level Waste (HLW) obtained from reprocessing of Spent Nuclear Fuel (SNF). A major focus is the separation of the minor actinides Am(III) and Cm(III) from lanthanides and other fission products with the interest of reducing the long-term heat generation of SNF.[8–10] The separation of particular metal ions is achieved by solvent extraction using selective hydrophilic or lipophilic ligands in aqueous and/or organic solutions, or a combination of ligands.[11] The main priority nowadays is looking for different ligands which can effectively separate actinides (An) from lanthanides (Ln) and Am from Cm.[12] Ideally, the ligands are composed of only C, H, O and N (the so-called CHON principle) which allows incinerating the final waste without generating additional solid waste. Diglycolamides (DGAs, *e.g.*, see Fig. 1) are molecules which contain two amide groups bound by an ether group. Since 2001, they have been tested for their capability to complex actinides and lanthanides in order to achieve the separation of minor An and Ln from HLW.[13] However, DGAs usually do not provide the required selectivity for An(III) over Ln(III). Therefore, they are often combined with other ligands in a synergistic system to enable the envisioned selective separation.[14,15]

A broad number of DGA derivatives with alkyl substituents on the amide groups have been synthesised and tested to assess their physical and chemical properties, specifically with f-elements.[13,16–18] The alkyl chains on the amide groups have a direct influence on the solubility of the ligand, *e.g.*, long alkyl chains (*n*-octyl and *n*-decyl) make the compounds lipophilic and present high distribution ratios from process relevant HNO_3 concentrations (1–6 mol L^{-1}) with An(III) and Ln(III). However, longer alkyl chains cause reduced distribution ratios due to steric hindrance.[13,17,19] On the other hand, short alkyl chains give hydrophilic DGAs. *N*,*N*,*N*′,*N*′-tetra-*n*-octyl diglycolamide (TODGA) and *N*,*N*,*N*′,*N*′-tetra-*n*-decyl diglycolamide (TDDGA) have been shown to be potential ligands for solvent extraction processes with high lipophilic solubility and high An(III) distribution ratios.[1,2,13,19,20] Afterwards, substituents on both methylene carbons in the backbone of the molecule with alkyl groups have been introduced to find that these groups

[a] *Forschungszentrum Jülich GmbH, Institut für Energie und Klimaforschung, Nukleare Entsorgung (IEK-6), 52428 Jülich, Germany. E-mail: a.wilden@fz-juelich.de*
[b] *Laboratory of Molecular Nanofabrication, Department for Molecules & Materials, Mesa+ Institute for Nanotechnology, University of Twente, 7500 AE Enschede, The Netherlands*

† Electronic supplementary information (ESI) available. See DOI: https://doi.org/10.1039/d2nj05663a

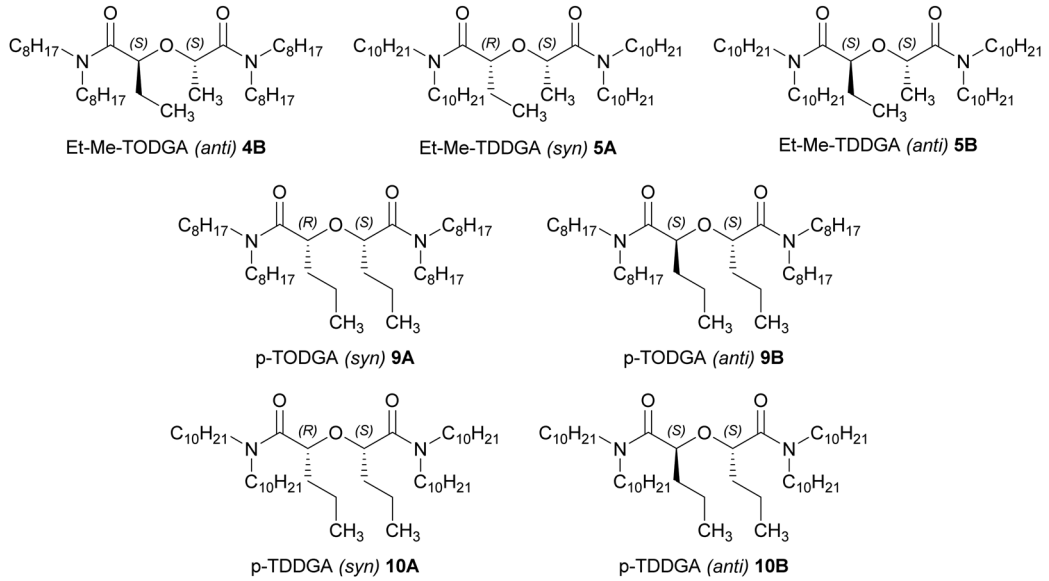

Fig. 1 Overview of the diglycolamide ligands used in this study with different alkyl side chain lengths (*n*-octyl and *n*-decyl), different substituents in the ligand backbone (dipropyl and ethyl-methyl), as well as different stereochemical orientation (*syn* or *anti*).

partly reduce radiolysis.[16,21–23] Another approach with interesting results concerns diastereomers of the doubly methylated TODGA derivative with methyl substitutions in the backbone.[24,25] Usually, DGAs present higher affinity for Cm over Am. For the methyl-substituted derivatives an inverse selectivity of Am over Cm by the Me_2-TODGA *anti*-diastereomer was observed, which was explained by the orientation influencing the interaction between the nitrate ions and the extracted metal complex.[23] Generally, the influence of the stereochemistry of extractants has yet only received little attention in the field of spent nuclear fuel treatment, despite the evidence on extraction differences caused by the orientation in ligands.[23,26–31] Based on these results, *n*-octyl and *n*-decyl DGAs were synthesised with dipropyl and ethyl-methyl substituents in the backbone of the molecules and their respective *syn*- and *anti*-isomers were isolated (Fig. 1), and their extraction behaviour and selectivity for An(III) and Ln(III), and specifically for Am(III) and Cm(III) was studied. Fundamental chemistry studies are planned on ligands with wider applicability. Here, the synthesis and first extraction studies were covered.

Results and discussion

The diastereomeric ligands **4, 5** and **9, 10** were prepared in an analogous way as described for Me_2-TODGA.[23] 2-Bromobutanoate was reacted with ethyl (*S*)-lactate in the presence of NaH as a base to give diastereomeric diesters **1** in a ratio of 3 : 1, which were separated by flash chromatography. Analogously, 2-bromovalerate was reacted with ethyl (±)-2-hydroxyvalerate to give diastereomeric diesters **6** in a ratio of 5 : 1. Saponification of the ester groups in **1** and **6** afforded the corresponding dicarboxylic acids **2** and **5** in quantitative yields. Using Schotten-Baumann conditions,[32] **2** and **5** were converted into the target compounds **4,5** and **9,10**, *via* the *in situ* prepared dichlorides, in varying yields.

In our previous study[23] we assigned the stereochemistry of the related Me_2-TODGA based on the difference in the ^{1}H NMR spectra upon complexation with lanthanum(III) triflate. In the ^{1}H NMR spectrum of the starting diester, the *anti*-diastereomer showed the $C(O)OCH_2$-signal as a quartet, as expected. However, in case of the *syn*-diastereomer the corresponding methylene group resides as a complicated multiplet due to steric interaction with the methyl group at the backbone. This characteristic feature is used for the assignment of the stereochemistry of the diesters **1** and **6**, showing the same characteristics, and consequently also holds for the ligands **4,5** and **9, 10**, respectively.

We expected low distribution ratios (*D*) associated with high uncertainties due to steric hindrance produced by the long alkyl side chains and the substitution of the methylene carbon atoms in the backbone. However, we are interested in the extraction behaviour and trends of each diastereomer and their affinity for Am(III) over Cm(III).[23] Distribution ratios were calculated as the ratio of activity or metal ion (M) concentration in the organic phase *vs.* the activity or metal ion concentration in the aqueous phase ($[M]_{org}/[M]_{aq}$) from single measurements. Fig. 2 shows the Am(III) distribution ratios for all synthesized ligands as a function of the nitric acid concentration. The first results of the ligand screening confirmed our predictions for the trivalent metal ions (*e.g.*, Am(III)). Distribution ratios increased with increasing HNO_3 concentration.[13] Generally, ethyl-methyl substitution for both alkyl side chain lengths (C8 and C10) extracted more Am(III) than for dipropyl substitution and regarding the orientation of the substituents in the backbone *syn*-diastereomers showed higher *D* values. The highest Am(III) *D* value was 7.0 for *syn*-Et-Me-TDDGA **5A** at 9.8 mol L^{-1} HNO_3. The *anti*-Et-Me-TDDGA **5B** diastereomer showed a distribution ratio of 5.5 at the same HNO_3 concentration. At lower HNO_3 concentrations the distribution ratios were approximately one to two orders of magnitude lower than for the *syn*

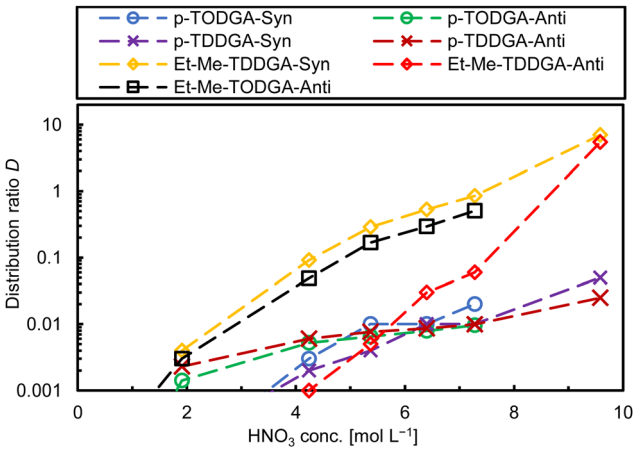

Fig. 2 Comparison of Am(III) distribution ratios for the different ligands used in this study. Org.: [Ligands] = 0.1 mol L^{-1} in *n*-dodecane; aq.: 10^{-5} mol L^{-1} Ln(III) (without Pm) + Y, Sr, Zr, Mo, Pd, Fe, Ru, ^{152}Eu, ^{239}Pu, ^{241}Am, ^{244}Cm; extraction time: 30 min, 22 °C.

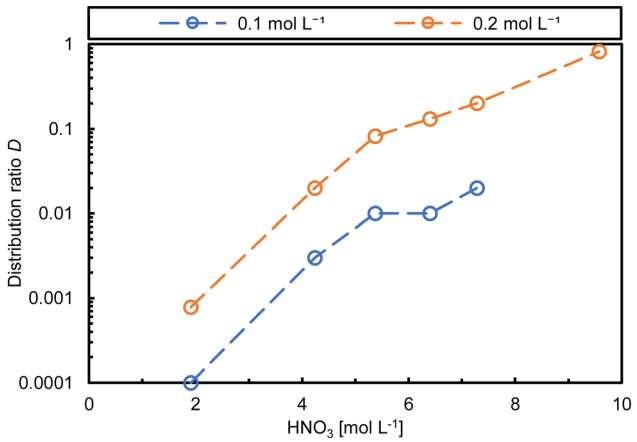

Fig. 3 ^{241}Am distribution ratios of *syn*-p-TODGA **9A** in two concentrations (exp. conditions see Fig. 2).

diastereomer. *Anti*-Et-Me-TODGA **4B** distribution ratios (Fig. 2, black squares) were close to but slightly lower than the ones of *syn*-Et-Me-TDDGA **5A** (Fig. 2, yellow diamonds). Even higher distribution ratios are expected for the *syn*-Et-Me-TODGA **4A** diastereomer as the *syn*-diastereomers of these diglycolamide extractants usually give higher distribution ratios than the *anti*-diastereomer.[23,30] However, the *syn*-Et-Me-TODGA **4A** diastereomer was synthetically unavailable and could not be tested in the current study. The differences in extraction by the different diastereomers was explained by the steric hindrance and orientation created by the alkyl groups of the ligand backbone hindering the nitrate ion complexation in the outer sphere of the complexes influencing their selectivity for Am(III) over Cm(III).[23,28–30]

The dipropyl substituted DGAs with the same orientation in both analogues showed similar behaviour. *Anti*-Orientation gave very low *D* values in a close range (0.005–0.009) slightly above the lower detection limit, without major differences among the HNO_3 concentration. *Syn*-Orientation gave only slightly higher *D* values at 4 to 7 mol L^{-1} nitric acid concentration. Hence, dipropyl substitutions present minimal differences on *D* ratios through the HNO_3 concentrations studied here.

The separation factor (SF) between two metal ions was calculated as the ratio of the corresponding distribution ratios ($SF_{M1/M2} = D_{M1}/D_{M2}$). As the SF is calculated from two *D* values with their individual uncertainties, best SF values are obtained where the corresponding *D* values are close to one. The separation factors reported here were determined accordingly. Concerning Am/Cm selectivity, the studied ligands showed a slight preference for Am(III) over Cm(III) with a separation factor of $SF_{Am/Cm} \sim 1.5$ (Fig. S1, ESI†). This finding is different from the behaviour of the two Me_2-TODGA diastereomers.[23] Our first hypothesis to explain this phenomenon is, that the overall steric hindrance by the longer alky chains of the ligands studied here compared to Me_2-TODGA might have a higher influence on Am(III)/Cm(III) selectivity compared to their orientation.

For all the ligands, process-relevant distribution ratios for the trivalent actinides >1 could only be achieved at very high HNO_3 concentrations of about 10 mol L^{-1}. Such high HNO_3 concentrations can cause splitting of the solvent phase into a light diluent rich phase with reduced extractant concentration, and a heavy phase containing complexes of HNO_3 with the extractant.[33,34] This 3rd phase formation phenomenon is undesirable for process applications. In other processes using diglycolamides (*e.g.*, TODGA) and high HNO_3 concentrations, a phase modifier like 1-octanol is used to mitigate 3rd phase formation.[33,35] According to literature, DGAs can form inverse micelles with polar molecules (*e.g.*, HNO_3) in long-chain alkane diluents (*e.g.*, *n*-dodecane or *n*-octane).[33,36,37] Massey *et al.* found that the addition of *n*-octanol reduced the degree of aggregation and hence reduced the degree of 3rd phase formation.[34] In our experiments, even at 10 mol L^{-1} HNO_3, no 3rd phase formation was observed. The steric hindrance from the substitution in the backbone seems to reduce the probability of increasing aggregate and cluster formation in solution, hence reducing the possibility of third-phase formation at high nitric acid concentrations.[33,34,37]

Low distribution ratios are not necessarily a disadvantage, as for a process application it must also be possible to back-extract the desired metal ions from the loaded organic phase. Nevertheless, the distribution ratios of the ligands considered here are quite low at a ligand concentration of 0.1 mol L^{-1} for the trivalent metal ions and associated with high uncertainties. Therefore, it is desirable to increase the distribution ratios maintaining the HNO_3 concentrations. Hence, the concentration of *syn-p*-TODGA **9A** was increased to 0.2 mol L^{-1} for 1.9–9.8 mol L^{-1} HNO_3. Distribution values indeed improved approx. 10-fold. Although, due to the dipropyl substitution, those values are still low compared to the moderate *D* values required ($D \geq 1$). Fig. 3 shows the comparison between 0.1 and 0.2 mol L^{-1} *syn*-p-TODGA **9A**.

Ethyl-methyl substitution in TODGA and TDDGA showed higher extraction for the Ln series (except Pm) and some FP compared to dipropyl substitution (see Fig. S2–S4, ESI†). For the other metal ions, *anti*-p-TODGA **9B** showed a higher extraction for Zr and Mo with values between 0.1 and 1 (Fig. S2–S3, ESI†), in comparison with *syn*-p-TODGA **9A** (*D* values below 0.1). On the other hand, Ru was not well extracted for most ligands

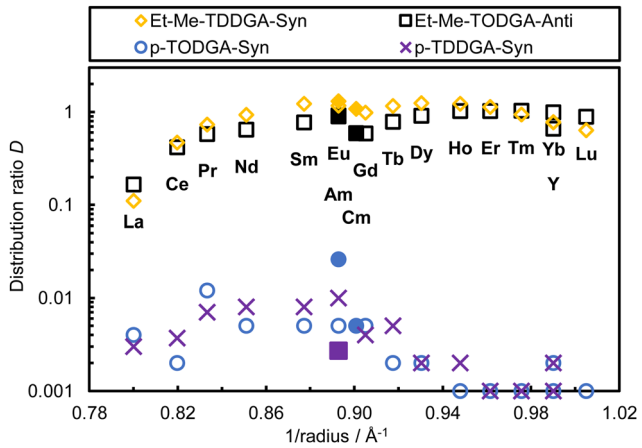

Fig. 4 Distribution ratios of Ln (w/o Pm, open symbols), Am and Cm (filled symbols) as a function of the inverse ionic radius for extraction at 7.4 mol L^{-1} HNO_3 (exp. conditions see Fig. 2).

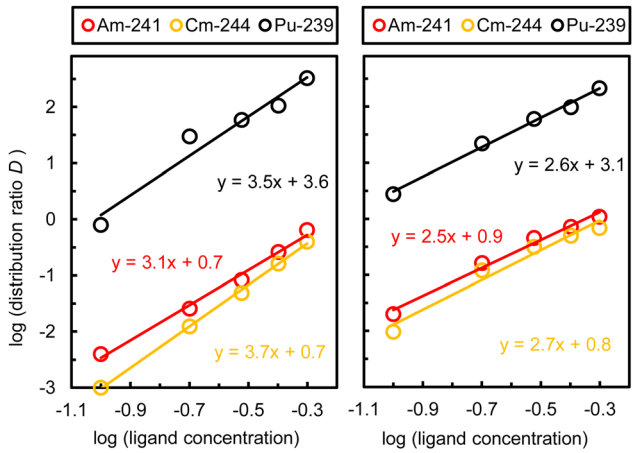

Fig. 6 Slope analysis for the extraction of $^{241}Am(III)$, $^{244}Cm(III)$ and $^{239}Pu(IV)$ by *anti*-p-TDDGA **10B** (left; aq. phase: 5.3 mol L^{-1} HNO_3) and *syn*-p-TODGA **9A** (right; aq. phase: 7.4 mol L^{-1} HNO_3). Org. phase: ligand concentrations 0.1–0.5 mol L^{-1}, Extraction time: 30 min, 22 °C.

(Fig. S4, ESI†), which is a positive effect since Ru most of the times is co-extracted complicating the system application.[17,36] Dipropyl substitution for TODGA and TDDGA *syn*-diastereomers showed poor extraction for Ln(III), independent of the HNO_3 concentration (Fig. 4). All metal ions were tested as radioactive spikes or in low concentrations (1×10^{-5} mol L^{-1}, each) to avoid loading, precipitation or 3rd phase formation. For further process development, these effects, and possible changes in the metal ions speciation (*e.g.*, Zr or Ru) would need to be studied.

Fig. 4 compares the distribution ratios of Ln(III) (except Pm) as a function of the inverse ionic radius[38,39] between ethyl-methyl and dipropyl substitutions. In this figure, the octad-effect is visible for *anti*-Et-Me-TODGA **4B** (Fig. 4, black squares) and *syn*-Et-Me-TDDGA **5A** (Fig. 4, yellow diamonds) contrary to the dipropyl analogues. The octad (2 curves each of 8 elements, including Gd in both) or tetrad-effects (four curves, each made of 4 elements, Gd is include in the 2nd and 3rd curve) observed in solvent extraction processes are due to half-filled f shells resulting in increased electronic stability.[40,41]

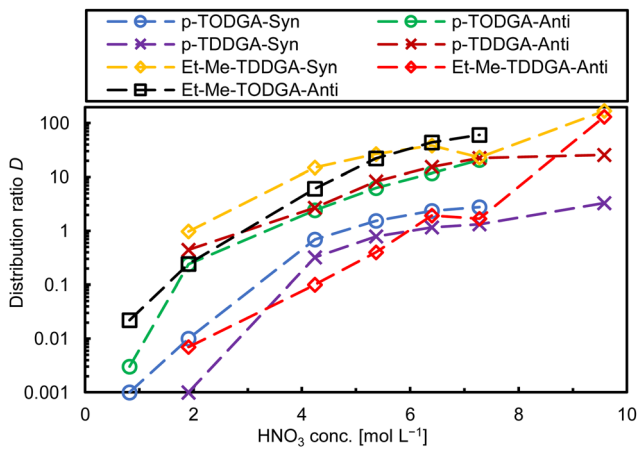

Fig. 5 Comparison of the Pu(IV) distribution ratios for the different ligands (exp. conditions see Fig. 2).

Pu(IV) extraction was tested to study the complexing behaviour of the newly synthesized DGAs with tetravalent actinide ions. Interestingly, in all cases, Pu(IV) was extracted with high distribution ratios. *Syn*-Et-Me-TDDGA **5A** (Fig. 5, yellow diamonds) and *anti*-Et-Me-TODGA **4B** Fig. 5, (black squares) gave the highest *D* values (see Fig. 5). Comparison of the different stereochemical orientation for the Et-Me or dipropyl substitutions gave different results for trivalent and tetravalent metal ions. For ethyl-methyl substitutions, the *syn* diastereomers showed better extraction, but interestingly, *anti*-dipropyl substitutions showed higher *D* values than their *syn*-analogues for Pu(IV).

The metal : ligand ratio was studied using slope analysis, assuming a solvation mechanism.[13] The slope of the log(*D*) *vs.* log(ligand concentration) plot then gives the number of ligand molecules per metal ion. For *anti*-p-TDDGA **10B**, we chose a nitric acid concentration of 5.3 mol L^{-1}, for *syn*-p-TODGA **9A** of 7.3 mol L^{-1} and varied the ligand concentration between 0.1 to 0.5 mol L^{-1}. Fig. 6 shows the logarithms of distribution ratios *vs.* ligand concentration at the fixed nitric acid concentration, including the results from the first extraction experiments at 0.1 mol L^{-1}. According with the linear trend, the slopes suggest approximately three ligand molecules per metal ion, which agrees well with the formation of 1 : 3 DGA complexes in the literature.[13,17,42,43]

Conclusions

A series of *syn*- and *anti*-diastereomers of novel backbone alkyl-substituted tetra-*n*-octyl and tetra-*n*-decyl diglycolamides was prepared and evaluated. Ethyl-methyl substitution for both diglycolamide groups (octyl and decyl side chains) gave the highest *D* values among the investigated molecules. However, these values were much lower than for their non-substituted parent molecules or for the methyl and dimethyl derivatives. Similarly, the dipropyl substitution for both extractants even further reduced the extraction of trivalent metal ions. Distribution ratios increased with increasing ligand concentration (tested only for the dipropyl substitutions) and

slope analysis confirmed a 1 : 3 metal : ligand ratio in accordance with the literature. However, the dipropyl substituted extractants give only low to moderate D values at high HNO_3 concentrations, which limits their possible application. The best results in the first screening were achieved with the ethyl–methyl substituted extractants, although still high HNO_3 concentrations were required. For further investigations, both diastereomers of Et-Me-TODGA need to be tested at a higher extractant concentration and reduced HNO_3 concentration, including additional spectroscopic and analytical techniques. All the studied diastereomers here showed a preference for Am over Cm, which was only observed for one other diglycolamide before. Although the observed Am/Cm separation factor is quite low here, understanding the fundamental effects causing the different selectivity of diglycolamides is crucial for the development of improved extractants and their application in solvent extraction processes. On the other hand, the ligands showed positive results for Pu(IV) extraction, which opens the possibility to use these ligands for separation of tetravalent ions from Ln(III) and other MA or in group actinide extraction processes.

Experimental

Reagents and solvents

All commercially available chemicals (Sigma-Aldrich, TCI, Chem-Pur, VWR) used in this study were analytical reagent grade and were used without further purification. All air sensitive reactions were carried out under nitrogen atmosphere using oven-dried glassware. All dry solvents were prepared according to standard procedures and stored over 3 or 4 Å molecular sieves.

Instrumentation and techniques

^{1}H NMR (Nuclear Magnetic Resonance) and ^{13}C NMR spectra were recorded on a Bruker Ascende™ 400 MHz NMR spectrometer (observation of ^{1}H at 400 MHz and of ^{13}C at 100 MHz). Partially deuterated solvents were used as internal standards to calculate the chemical shifts (d values in ppm). All ^{13}C NMR spectra were performed with proton decoupling. The used abbreviations in these spectra are singlet (s), doublet (d), triplet (t), quadruplet (q), quintet (quint) and multiplet (m). IR spectra were recorded on an FT-IR spectrometer (Thermo Scientific Nicolet 6700) with a diamond ATR accessory (Thermo Optec Smart Orbit). Electrospray ionization (ESI) mass analyses were performed on a Waters micromass LCT mass spectrometer SQ Detector in positive mode using MeOH or CH_3CN as solvents.

To monitor the progress of reactions, aluminum sheets covered with silica gel 60 F-254 provided by Merck were used. All aluminum sheets were revealed under an ultraviolet lamp (λ = 254 nm) or using staining reagents.

The characterization data of the individual compounds from ^{1}H and ^{13}C NMR, as well as FT-IR and ESI-MS spectrometry are given in the ESI.†

Procedures

Scheme 1 shows the corresponding structures and synthesis pathway of the tetra n-octyl and n-decyl DGAs with ethyl, methyl

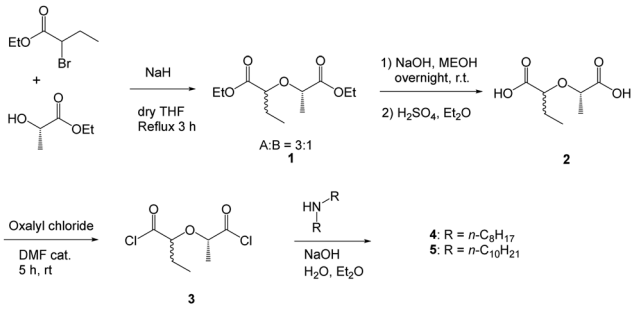

Scheme 1 Synthesis of Et-Me-TODGA **4** and Et-Me-TDDGA **5**.

substituents in the backbone. During the synthesis several times there was treatment with acid (20% sulfuric acid and oxalyl chloride, the latter one generating HCl). Never any racemization was observed.

Ethyl (*R*)-2-(((*S*)-1-ethoxy-1-oxopropan-2-yl)oxy)butanoate (1A) and ethyl (*S*)-2-(((*S*)-1-ethoxy-1-oxopropan-2-yl)oxy)butanoate (1B). A suspension of sodium hydride (60% in oil; 2.2 g, 55 mmol) in n-hexane (10 mL) was stirred for 15 min, whereupon the solvent was removed using a pipette. Dry THF (20 mL) was added, and the suspension was cooled to 0 °C using an ice bath. Then, a solution of ethyl (*S*)-lactate (5.7 mL, 50 mmol) in dry THF and of racemic ethyl 2-bromobutanoate (7.3 mL, 50 mmol) were added dropwise and sequentially. The mixture was stirred at room temperature for 1 h and then refluxed for 3 h. After evaporation of the solvent under reduced pressure the crude mixture was dissolved in water (50 mL) and the aqueous phase extracted with Et_2O (3 × 50 mL). The combined organic phases were washed with brine (50 mL) and dried over anhydrous $MgSO_4$. The solvent was evaporated in vacuum to obtain a yellowish liquid. Purification by flash column chromatography using n-heptane/AcOEt 3 : 1 afforded diastereomer **1A** and diastereomer **1B** in 53% and 17% yield, respectively.

(*R*)-2-((*S*)-1-Carboxyethoxy)butanoic acid (2A). A solution of diester **1A** (2.66 g, 11.45 mmol) and NaOH (2.6 g, 65 mmol) in MeOH (50 mL) was stirred overnight. Then, the solvent was evaporated under reduced pressure and the white solid obtained was kept under high vacuum to completely remove the solvent. The flask was cooled using an ice bath and cold 20% H_2SO_4 were added dropwise. The aqueous phase was extracted with Et_2O (3 × 50 mL) whereupon the combined organic phases were dried over anhydrous $MgSO_4$. The solvent was removed under vacuum to obtain the product in quantitative yield.

(*S*)-2-((*S*)-1-Carboxyethoxy)butanoic acid (2B). It was prepared following the same procedure as for **2A**, starting from diester **1B** (0.76 g, 3.27 mmol) and NaOH (0.75 g, 18.7 mmol) in MeOH (20 mL). The solvent was removed under vacuum to obtain the product in quantitative yield.

General procedure for the *in situ* preparation of diacyl chlorides 3A,B and 8A,B

To a solution of a substituted dicarboxylic acid (1 mmol) dissolved in pure oxalyl chloride (2 mL), DMF (some drops) was added. The mixture was stirred under nitrogen for 4 hours, whereupon the oxalyl chloride was removed under vacuum. The

product was obtained in quantitative yield and immediately dissolved in Et_2O to be used for the synthesis of DGAs.

(*S*)-2-(((*S*)-1-(Di-*n*-octylamino)-1-oxopropan-2-yl)oxy)-*N*,*N*-di-*n*-octylbutanamide (4B). A solution of diglycolyl chloride **3B** (0.5 g, 2.44 mmol) in Et_2O (20 mL) was added dropwise to a solution of di-*n*-octylamine (1.5 g, 6.1 mmol) in 0.8 mol L^{-1} NaOH (40 mL) at 0 °C over 30 min. The mixture was stirred at 0 °C for 2 h, then the phases were separated. The aqueous layer was extracted with Et_2O (3 × 20 mL). 10% HCl (20 mL) was added to the combined organic layers and the solution was shaken vigorously to form clumps of ammonium salts which were filtered off. The organic layer was washed with 10% HCl (2 × 30 mL) then filtered through a glass frit (G3) when necessary. A poly(4-styrenesulfonic acid) solution in water (20 mL) was added to the organic layer. The mixture was shaken vigorously to form polymeric salts as an amorphous material floating between the layers. The organic layer was washed three times with water and then separated from the polymeric salt. It was dried over anhydrous $MgSO_4$ and the solvent was evaporated under vacuum to afford a viscous oil. The crude mixture was purified by flash column chromatography using *n*-heptane/AcOEt 1 : 1 as eluent to give the product as a yellowish oil in 42% yield.

(*R*)-*N*,*N*-Di-*n*-decyl-2-(((*S*)-1-(*N*,*N*-di-*n*-decylamino)-1-oxopropan-2-yl)oxy)butanamide (5A). A solution of diglycolyl chloride **3A** (1.5 g, 7.04 mmol) in Et_2O (60 mL) was added dropwise to a solution of di-*n*-decylamine (5.24 g, 17.6 mmol) in 0.8 mol L^{-1} NaOH (60 mL) at 0 °C over 30 min. The mixture was stirred at 0 °C for 2 h, then the phases were separated. The aqueous layer was extracted with Et_2O (3 × 30 mL). 10% HCl (20 mL) was added to the combined organic phases and the solution was shaken vigorously to form clumps of ammonium salts, which were filtered off. The organic layer was washed with 10% HCl (2 × 30 mL) and then filtered through a glass frit (G3) when necessary. A poly(4-styrenesulfonic acid) solution in water (10 mL) was added to the organic layer. The mixture was shaken vigorously to form polymeric salts as an amorphous material floating between the layers. The organic layer was washed three times with water and then separated from the polymeric salt. It was dried over anhydrous $MgSO_4$ and the solvent was evaporated under vacuum to afford a viscous oil. The crude mixture was purified by flash column chromatography using *n*-heptane/AcOEt 1 : 1 as eluent. The product was obtained as a yellowish oil in 30% yield.

(*S*)-*N*,*N*-Di-*n*-decyl-2-(((*S*)-1-(*N*,*N*-di-*n*-decylamino)-1-oxopropan-2-yl)oxy)butanamide (5B). A solution of diglycolyl chloride **3B** (1.6 g, 7.5 mmol) in Et_2O (50 mL) was added dropwise to a solution of di-*n*-decylamine (5.6 g, 18.8 mmol) in 0.8 mol L^{-1} NaOH (50 mL) at 0 °C over 30 min. Following the procedure as for **5A** gave **5B** as a yellowish oil in 23% yield.

Scheme 2 shows the corresponding structures and synthesis pathway scheme of the tetra *n*-octyl and *n*-decyl DGAs with *n*-propyl substituents in the backbone.

Diethyl 2,2′-oxydipentanoate (6A and 6B). A suspension of sodium hydride (1.5 g, 37.6 mmol) in *n*-hexane (10 mL) was stirred for 15 min, whereupon the solvent was removed using a pipette. Dry THF (20 mL) was added, and the suspension was cooled to 0 °C using an ice bath. Then, a solution of ethyl (±)-2-hydroxyvalerate (5.0 g, 34.2 mmol) in dry THF and of ethyl 2-bromovalerate (7.15 g, 34.2 mmol) were added dropwise and sequentially. The mixture was stirred at room temperature for 1 h and then refluxed for 3 h. The solvent was evaporated under reduced pressure. The crude was dissolved in water (50 mL) and the aqueous phase extracted with Et_2O (3 × 50 mL). The combined organic layers were washed with brine (50 mL) and dried over anhydrous $MgSO_4$. The solvent was evaporated in vacuum to obtain a yellowish liquid. It was purified by flash column chromatography using *n*-heptane/AcOEt 9 : 1 as eluent. Diastereomer **A** was obtained in 59% yield and diastereomer **B** in 11% yield.

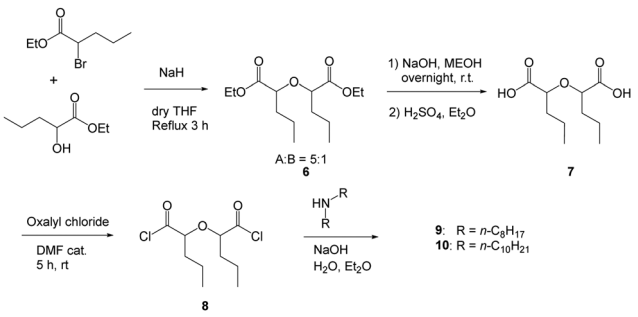

Scheme 2 Synthesis of p-TODGA **9** and p-TDDGA **10**.

2,2′-Oxydipentanoic acid (7A). A solution of diethyl 2,2′-oxydipentanoate **6A** (4.2 g, 15.3 mmol) and NaOH (3.4 g, 85.7 mmol) in MeOH (80 mL) was stirred overnight. Then, the solvent was evaporated under reduced pressure and the white solid obtained was kept under high vacuum to completely remove the solvent. The flask was cooled using an ice bath and cold 20% H_2SO_4 (20 mL) were added dropwise. The aqueous phase was extracted with Et_2O (3 × 50 mL) then the combined organic phases were dried over anhydrous $MgSO_4$. The solvent was removed under vacuum to obtain the product in quantitative yield.

2,2′-Oxydipentanoic acid (7B). It was prepared following the same procedure as for 2,2′-oxydipentanoic acid **7A**, starting from diethyl 2,2′-oxydipentanoate **6B** (0.76 g, 3.27 mmol) and NaOH (0.75 g, 18.7 mmol) in MeOH (20 mL). The solvent was removed under reduced pressure to afford the product in quantitative yield.

2,2′-Oxybis(*N*,*N*-di-*n*-octylpentanamide) (9A). A solution of diglycolyl chloride **8A** (3.2 g, 12.5 mmol) in Et_2O (90 mL) was added dropwise to a solution of di-*n*-octylamine (76 g, 31.3 mmol) in 0.8 mol L^{-1} NaOH (100 mL) at 0 °C over 30 min. The mixture was stirred at 0 °C for 2 h and then the phases were separated. The aqueous layer was extracted with Et_2O (3 × 50 mL). 10% HCl (40 mL) was added to the combined organic layers and the solution was shaken vigorously to form clumps of ammonium salts, which were filtered off. The organic layer was washed with 10% HCl (2 × 30 mL) and subsequently filtered through a glass frit (G3) when necessary. A poly(4-styrenesulfonic acid) solution in water (20 mL) was added to the organic layer. The mixture was shaken vigorously

to form polymeric salts as an amorphous material floating between the layers. The organic layer was washed three times with water and then separated from the polymeric salt. It was dried over anhydrous $MgSO_4$ and the solvent was evaporated under vacuum to afford a viscous oil. It was purified by flash column chromatography using *n*-heptane/AcOEt 8 : 2 as eluent. The product was obtained as a yellowish oil in 54% yield.

2,2′-Oxybis(*N*,*N*-di-*n*-octylpentanamide) (9B). A solution of diglycolyl chloride **8B** (0.8 g, 3.13 mmol) in Et_2O (25 mL) was added dropwise to a solution of di-*n*-octylamine (1.9 g, 7.8 mmol) in 0.8 mol L^{-1} NaOH (25 mL) at 0 °C over 30 min. The mixture was stirred at 0 °C for 2 h, whereupon the phases were separated. The aqueous layer was extracted three times (3 × 20 mL) with Et_2O. 10% HCl (20 mL) was added to the combined organic phases. The rest of the procedure is identical to that of **9A**, ultimately giving **9B** as a yellowish oil in 24% yield.

2,2′-Oxybis(*N*,*N*-di-*n*-decylpentanamide) (10A). A solution of diglycolyl chloride (1.1 g, 4.3 mmol) in Et_2O (40 mL) was added dropwise to a solution of di-*n*-decylamine (3.2 g, 10.7 mmol) in 0.8 mol L^{-1} NaOH (40 mL) at 0 °C over 30 min. The mixture was stirred at 0 °C for 2 h then the phases were separated. The aqueous layer was extracted three times (30 mL) with Et_2O. 10% HCl (20 mL) was added to the combined organic phases and the solution was shaken vigorously to form clumps of ammonium salts which were filtered off. The organic layer was washed with 10% HCl (2 × 20 mL) then filtered through a glass frit (G3) when necessary. A poly(4-styrenesulfonic acid) solution in water (20 mL) was added to the organic layer. The mixture was shaken vigorously to form polymeric salts as an amorphous material floating between the layers. The organic layer was washed three times with water and then separated from the polymeric salt. It was dried over anhydrous $MgSO_4$ and the solvent was evaporated under vacuum to afford a viscous oil. It was purified by flash column chromatography using *n*-heptane/AcOEt 9 : 1 as eluent. The product was obtained as a yellowish oil in 45% yield.

2,2′-Oxybis(*N*,*N*-di-*n*-decylpentanamide) (10B). A solution of diglycolyl chloride **8B** (1.3 g, 5.3 mmol) in Et_2O (40 mL) was added dropwise to a solution of di-*n*-decylamine (3.9 g, 13.2 mmol) in 0.8 mol L^{-1} NaOH (40 mL) at 0 °C over 30 min. Following the same procedure as for **10A** afforded a viscous oil. It was purified by flash column chromatography using *n*-heptane/AcOEt 8 : 2 as eluent to give **10B** as a yellowish oil in 50% yield.

Solvent extraction

Nitric acid dilutions (HNO_3, Merck AG, 0.82–9.78 mol L^{-1}) were prepared using ultra-pure water (18.2 MΩ cm) which was obtained from an Elga Purelab Ultra water purification system. The radiotracers ^{241}Am, ^{244}Cm and ^{152}Eu were purchased from Isotopendienst M. Blaseg GmbH, Waldburg, Germany, Oak Ridge National Laboratory, Oak Ridge, USA, and Eckert & Ziegler Nuclitec GmbH, Braunschweig, Germany, respectively. ^{239}Pu tracer was used from a laboratory stock solution. The Pu oxidation state in the stock solution was Pu(IV) as confirmed by UV/Vis spectroscopy with ≤5% Pu(VI). The oxidation state was not checked during or after extraction, as the Pu concentration in the extraction samples was too low. Nevertheless, under the applied extraction conditions (high nitric acid concentrations and short extraction time at 22 °C) the formation of other than Pu(IV) oxidation states is highly unlikely.[44–47] For the screening experiments diluted metal ion solutions (Fe, Sr, Y, Zr, Mo, Ru, Pd, La, Ce, Pr, Nd, Sm, Eu, Gd, Tb, Dy, Ho, Er, Tm, Yb, Lu) in HNO_3 were used with metal ion concentrations of 1×10^{-5} mol L^{-1}, each, to avoid loading, precipitation or 3rd phase formation. Acid concentration was measured by titration against 0.1 mol L^{-1} NaOH using a Titrando 907, purchased from Metrohm GmbH & Co. KG (Filderstadt, Germany). All chemicals were used without further purification. Organic solutions of 0.1 mol L^{-1} DGA were prepared using a weighed quantity of ligand in *n*-dodecane (Sigma Aldrich).

Procedures and analytics

Batch solvent extraction experiments were carried out using equal volumes of 500 μL of each phase. The aqueous and organic phases were pipetted into screw-cap glass vials and contacted for a given time on an IKA VIBRAX VXR, IKA®-Werke GmbH & Co. KG (Staufen, Germany) basic automatic shaker at 2,200 rpm and 22 °C. The temperature was controlled by a F25-HE thermostat, JULABO GmbH (Seelbach, Germany). After mixing, the samples were centrifuged with a Hettich EBA 8s centrifuge, Andreas Hettich GmbH & Co. KG (Tuttlingen, Germany), for 5 min. The phases were then separated manually using a fine tipped transfer micropipette. 200 μL of each phase were transferred into new glass vials for further measurements.

Gamma measurements of ^{241}Am (60 keV) and ^{152}Eu (122 keV) were carried out using an Eurisys EGC 35-195-R germanium coaxial N-type detector and spectra were evaluated using the GammaVision Software. Samples were measured directly without further treatment of the samples. Alpha measurements were carried out for ^{239}Pu (5157 keV), ^{241}Am (5486 keV) and ^{244}Cm (5805 keV) using an Ortec/Ametek ALPHA-ENSEMBLE-8 eight chamber alpha measurement system equipped with PIPS detectors purchased from Ametek GmbH (Meerbusch, Germany). Sample preparation for alpha measurement was done by homogenizing a 10 μL alpha-spectroscopy sample in 100 μL of a mixture of Zapon varnish and acetone (1 : 100 v/v). This mixture was distributed over a stainless-steel plate obtained from Berthold, Bad Wildbad, Germany. The sample was dried under a heating lamp and annealed into the stainless-steel plate by a gas-flame burner. For stable elements, Inductively Coupled Plasma Mass Spectrometry (ICP-MS) was applied using a PerkinElmer NexION 2000C. Aqueous samples were measured after dilution in 1% v/v nitric acid solution without further treatment. Organic samples were measured directly in a tenside matrix (Triton-X-100) in 1% v/v HNO_3 after dilution.

Distribution ratios (D) were calculated as the ratio of activity or metal ion (M) concentration in the organic phase *vs.* the activity or metal ion concentration in the aqueous phase ($[M]_{org}/[M]_{aq}$). The separation factor (SF) between two metal ions was calculated as the ratio of the corresponding distribution ratios ($SF_{M1/M2} = D_{M1}/D_{M2}$). Distribution ratios between

0.01 and 100 exhibit an uncertainty of ±5%, while lower/higher values exhibit larger uncertainties, yet they represent the complexing trend of the ligands. Mass balances were calculated as the sum of aqueous and organic concentrations divided by the initial concentration.

Conflicts of interest

There are no conflicts to declare.

Acknowledgements

Funding for this research was provided by the German Federal Ministry for the Environment, Nature Conservation, Nuclear Safety and Consumer Protection (BMUV), project SEPAM (02E11921A).

References

1 A. Wilden, G. Modolo, P. Kaufholz, F. Sadowski, S. Lange, M. Sypula, D. Magnusson, U. Müllich, A. Geist and D. Bosbach, *Solvent Extr. Ion Exch.*, 2015, **33**, 91–108.
2 C. Wagner, U. Müllich, A. Geist and P. J. Panak, *Solvent Extr. Ion Exch.*, 2016, **34**, 103–113.
3 M. Miguirditchian, L. Chareyre, X. Heres, C. Hill, P. Baron and M. Masson, *Global, 2007, Advanced Nuclear Fuel Cycles and Systems*, Boise, ID, United States, 2007.
4 R. Malmbeck, M. Carrott, B. Christiansen, A. Geist, X. Hérès, D. Magnusson, G. Modolo, C. Sorel, R. Taylor and A. Wilden, *Sustainable Nuclear Energy Conference*, Manchester, UK, 2014.
5 M. Carrott, K. Bell, J. Brown, A. Geist, C. Gregson, X. Hères, C. Maher, R. Malmbeck, C. Mason, G. Modolo, U. Müllich, M. Sarsfield, A. Wilden and R. Taylor, *Solvent Extr. Ion Exch.*, 2014, **32**, 447–467.
6 A. Geist, J.-M. Adnet, S. Bourg, C. Ekberg, H. Galán, P. Guilbaud, M. Miguirditchian, G. Modolo, C. Rhodes and R. Taylor, *Sep. Sci. Technol.*, 2021, **56**, 1866–1881.
7 T. L. Authen, J.-M. Adnet, S. Bourg, M. Carrott, C. Ekberg, H. Galán, A. Geist, P. Guilbaud, M. Miguirditchian, G. Modolo, C. Rhodes, A. Wilden and R. Taylor, *Sep. Sci. Technol.*, 2022, **57**, 1724–1744.
8 E. M. González-Romero, *Nucl. Eng. Des.*, 2011, **241**, 3436–3444.
9 T. Kooyman, *Ann. Nucl. Energy*, 2021, **157**, 7.
10 OECD-NEA, *Strategies and Considerations for the Back End of the Fuel Cycle*, OECD Nuclear Energy Agency (NEA), Boulogne-Billancourt, France, 2021.
11 *Ion Exchange and Solvent Extraction: Changing the Landscape in Solvent Extraction*, ed. B. A. Moyer, CRC Press, Taylor & Francis Group, Boca Raton, Fl, USA, 2020.
12 OECD-NEA, *Potential Benefits and Impacts of Advanced Nuclear Fuel Cycles with Actinide Partitioning and Transmutation*, Report NEA No. 6894, OECD, *Nuclear Energy Agency (NEA)*, 2011.
13 Y. Sasaki, Y. Sugo, S. Suzuki and S. Tachimori, *Solvent Extr. Ion Exch.*, 2001, **19**, 91–103.
14 P. J. Panak and A. Geist, *Chem. Rev.*, 2013, **113**, 1199–1236.
15 P. Matveev, P. K. Mohapatra, S. N. Kalmykov and V. Petrov, *Solvent Extr. Ion Exch.*, 2021, **39**, 679–713.
16 M. Iqbal, J. Huskens, W. Verboom, M. Sypula and G. Modolo, *Supramol. Chem.*, 2010, **22**, 827–837.
17 S. A. Ansari, P. Pathak, P. K. Mohapatra and V. K. Manchanda, *Chem. Rev.*, 2012, **112**, 1751–1772.
18 Y. Y. Liu, C. Zhao, Z. B. Liu, S. Liu, Y. Zhou, C. S. Jiao, M. Zhang, Y. Gao, H. He and S. W. Zhang, *RSC Adv.*, 2022, **12**, 790–797.
19 S. A. Ansari, P. N. Pathak, V. K. Manchanda, M. Husain, A. K. Prasad and V. S. Parmar, *Solvent Extr. Ion Exch.*, 2005, **23**, 463–479.
20 J. Brown, F. McLachlan, M. J. Sarsfield, R. J. Taylor, G. Modolo and A. Wilden, *Solvent Extr. Ion Exch.*, 2012, **30**, 127–141.
21 H. Galán, C. A. Zarzana, A. Wilden, A. Núñez, H. Schmidt, R. J. M. Egberink, A. Leoncini, J. Cobos, W. Verboom, G. Modolo, G. S. Groenewold and B. J. Mincher, *Dalton Trans.*, 2015, **44**, 18049–18056.
22 V. Hubscher-Bruder, V. Mogilireddy, S. Michel, A. Leoncini, J. Huskens, W. Verboom, H. Galán, A. Núñez, J. Cobos Sabate, G. Modolo, A. Wilden, H. Schmidt, M.-C. Charbonnel, P. Guilbaud and N. Boubals, *New J. Chem.*, 2017, **41**, 13700–13711.
23 A. Wilden, P. M. Kowalski, L. Klaß, B. Kraus, F. Kreft, G. Modolo, Y. Li, J. Rothe, K. Dardenne, A. Geist, A. Leoncini, J. Huskens and W. Verboom, *Chem. – Eur. J.*, 2019, **25**, 5507–5513.
24 B. Verlinden, K. Van Hecke, A. Wilden, M. Hupert, B. Santiago-Schübel, R. J. M. Egberink, W. Verboom, P. M. Kowalski, G. Modolo, M. Verwerft, K. Binnemans and T. Cardinaels, *RSC Adv.*, 2022, **12**, 12416–12426.
25 B. Verlinden, A. Wilden, K. Van Hecke, R. J. M. Egberink, J. Huskens, W. Verboom, M. Hupert, P. Wessling, A. Geist, P. J. Panak, R. Hermans, M. Verwerft, G. Modolo, K. Binnemans and T. Cardinaels, *Solvent Extr. Ion Exch.*, 2023, **41**, 59–87.
26 A. H. Bond, R. Chiarizia, V. J. Huber, M. L. Dietz, A. W. Herlinger and B. P. Hay, *Anal. Chem.*, 1999, **71**, 2757–2765.
27 A. M. Costero, J. P. Villarroya, S. Gil, M. J. Aurell and M. C. R. de Arellano, *Tetrahedron*, 2002, **58**, 6729–6734.
28 Y. Lin, J. Espinas, S. Pellet-Rostaing, A. Favre-Reguillon and M. Lemaire, *New J. Chem.*, 2010, **34**, 388–390.
29 F. L. Guerra Gomez, T. Uehara, T. Rokugawa, Y. Higaki, H. Suzuki, H. Hanaoka, H. Akizawa and Y. Arano, *Bioconjugate Chem.*, 2012, **23**, 2229–2238.
30 N. Felines, G. Arrachart, F. Giusti, A. Beillard, C. Marie and S. Pellet-Rostaing, *New J. Chem.*, 2021, **45**, 12798–12801.
31 P. Wessling, M. Trumm, T. Sittel, A. Geist and P. J. Panak, *Radiochim. Acta*, 2022, **110**, 291–300.
32 A. Leoncini, J. Huskens and W. Verboom, *Synlett*, 2016, 2463–2466.

33 T. Yaita, A. W. Herlinger, P. Thiyagarajan and M. P. Jensen, *Solvent Extr. Ion Exch.*, 2004, **22**, 553–571.
34 D. Massey, A. Masters, J. Macdonald-Taylor, D. Woodhead and R. Taylor, *J. Phys. Chem. B*, 2022, **126**, 6290–6300.
35 A. Geist, U. Müllich, D. Magnusson, P. Kaden, G. Modolo, A. Wilden and T. Zevaco, *Solvent Extr. Ion Exch.*, 2012, **30**, 433–444.
36 J. Ravi, K. A. Venkatesan, M. P. Antony, T. G. Srinivasan and P. R. Vasudeva Rao, *Radiochim. Acta*, 2013, **101**, 301.
37 P. Narayanan, K. R. Swami, T. Prathibha and K. A. Venkatesan, *ChemistrySelect*, 2022, **7**, 11.
38 P. D'Angelo, A. Zitolo, V. Migliorati, G. Chillemi, M. Duvail, P. Vitorge, S. Abadie and R. Spezia, *Inorg. Chem.*, 2011, **50**, 4572–4579.
39 P. D'Angelo, F. Martelli, R. Spezia, A. Filipponi and M. A. Denecke, *Inorg. Chem.*, 2013, **52**, 10318–10324.
40 D. F. Peppard, G. W. Mason and S. Lewey, *J. Inorg. Nucl. Chem.*, 1969, **31**, 2271–2272.
41 T. Monecke, U. Kempe, J. Monecke, M. Sala and D. Wolf, *Geochim. Cosmochim. Acta*, 2002, **66**, 1185–1196.
42 Y. Sasaki, P. Rapold, M. Arisaka, M. Hirata, T. Kimura, C. Hill and G. Cote, *Solvent Extr. Ion Exch.*, 2007, **25**, 187–204.
43 A. Wilden, G. Modolo, S. Lange, F. Sadowski, B. B. Beele, A. Skerencak-Frech, P. J. Panak, M. Iqbal, W. Verboom, A. Geist and D. Bosbach, *Solvent Extr. Ion Exch.*, 2014, **32**, 119–137.
44 Y. Ban and Y. Morita, *Radiochim. Acta*, 2012, **100**, 879–883.
45 M. H. Lee, Y. J. Park and W. H. Kim, *J. Radioanal. Nucl. Chem.*, 2007, **273**, 375–382.
46 *The Chemistry of the Actinide and Transactinide Elements*, ed. L. R. Morss, N. M. Edelstein and J. Fuger, Springer, Dordrecht, The Netherlands, 4th edn, 2011.
47 J. M. Cleveland, *The Chemistry of plutonium*, American Nuclear Society, La Grange Park, IL, Reprint of the 1970 ed. published by Gordon and Breach, New York; with new pref. and foreword edn., 1979.